Adaptive parameter selection for gradient-sparse + low patch-rank recovery: application to image decomposition

Antoine Guennec, Jf Aujol, Yann Traonmilin

Adaptive parameter selection for gradient-sparse plus low patch-rank recovery: application to image decomposition

Antoine Guennec
Institut de Mathématique de Bordeaux
Bordeaux, France
antoine.guennec@math.u-bordeaux.fr

Jean-François Aujol
Institut de Mathématique de Bordeaux
Bordeaux, France
Jean-Francois.Aujol@math.u-bordeaux.fr

Yann Traonmilin
Institut de Mathématique de Bordeaux
Bordeaux, France
yann.traonmilin@math.u-bordeaux.fr

***Abstract*—In this work, we are interested in gradient sparse plus low patch-rank signal recovery for image structure-texture decomposition, the structure being gradient-sparse and the texture low patch-rank. Based upon theoretical results of sparse plus low-rank matrix recovery, we propose an algorithm to automatically tune the regularization parameters of our model depending on the content of the image. This permits to provide an improved localized version of gradient sparse plus low patch-rank decomposition. This algorithm is validated by experiments on synthetic and real images.**

***Index Terms*—Image decomposition, cartoon, texture, optimization, gradient-sparsity, low patch-rank**

I. Introduction

The problem of decomposing an image into a structure/cartoon component and a texture component has been a longstanding area of research, with an extensive number of applications such as image restoration, pattern recognition, deraining and astromical imaging. The problem is typically given as follows: given an image f, find a decomposition $f = u+v$ such that u is a is piecewise constant approximation of the image, called the structure or cartoon component, and v is zero-mean, oscillating and with local patterns, called the texture component. The problem is notoriously ill-posed as there are twice more unknowns than known variables. Furthermore, parameter tuning in structure-texture decomposition, the focus of this paper, is notoriously difficult as the tuning parameters depend upon the content of each image.

The problem of structure-texture decomposition (STD) is often formulated as an optimization problem of the form

$$\min_{\substack{u,v \\ f=u+v}} \mu R_1(u) + \gamma R_2(v), \tag{1}$$

where μ, γ are the tuning parameters and R_1, R_2 are the regularization functions for the structure and texture components respectively. For the characterization of the structure component, most models use the total variation [1], $R_1(u) = \|u\|_{TV} = \|\nabla u\|_1$, since it characterizes well the piecewise constant nature of the structure component. Although the choice of the characterization of the structural component has remained relatively unchanged across most proposed STD models, many options exist when it comes to the texture component.

Historically the first STD variational-based models use the total variation to characterize the structural component, and they use a functional space norm to constrain the textural component, such as the L2-norm [1], G-norm [2], [3], L1-norm [4] or $\mathcal{H}$-norm [5], [6]. While theoretically well-founded and able to capture the oscillating nature of texture, these norms are either difficult to implement or cannot capture textures with a small magnitude.

More recently, learning based approaches have been proposed. In [7] the authors proposed a self-example and unsupervised learning approach where the STD functional is optimized using a neural network. In [8]–[10], methods based upon unfolding the TV proximal operator have been proposed.

In the category of sparsity-prior and low-rank prior, the texture is considered to be sparsely represented in an appropriate dictionary, which is either fixed or learned. One of the earliest approach on the subject was to consider that texture can be sparsely represented in a suitable given transformation (e.g discrete cosine transform (DCT), Gabor transform) [11], [12]. While very successful in some applications, the issue with this approach is that many textures that arise in practical applications cannot be modeled by DCT or other related dictionaries. More recently, this approach was extended to use convolutional sparse coding instead [13], where convolutional filters are learned beforehand. However, this method is dependent on the resolution thus the learned convolutional filters should be trained accordingly.

The approach that we lean on in this paper is Schaeffer and Osher's low-patch rank (LPR) model [14] in which the texture is considered to be of low patch-rank. That is to say that given a patch map $\mathcal{P} : \mathbb{R}^{n\times m} \to \mathbb{R}^{p^2\times N}$ (with overlap), where $p \times p$ is the dimension of the patches and N the number of extracted patches from the image, $\text{rank}(\mathcal{P}(v))$ should be relatively small. Conceptually, this expresses the idea that patches of textures should reside within a common small vector space. However, as rank-minimization is well known to be a NP-hard problem, we instead minimize the

nuclear norm $R_2(v) = \|\mathcal{P}(v)\|_* = \sum_i \sigma_i(\mathcal{P}(v))$, which is known to enforce low rank. As such, the (LPR) model is written as

$$\min_{\substack{u,v \\ f=u+v}} \mu \|\nabla u\|_1 + \gamma \|\mathcal{P}(v)\|_* , \tag{2}$$

where μ and γ are the tuning parameters. This optimization problem can be solved using the *Alternating Direction Method of Multiplier* (ADMM) [15]. While the LPR model is more capable of extracting ideal textures from an image with well-patterned texture than previous models, the fact that it uses the nuclear norm to capture the low rank of patches of the texture globally is an issue, notably when the given image contains many different texture patterns. More recently, Ono et al. [16] proposed a blockwise low-rank texture model (BNN) to counteract against this issue with LPR.

While these methods yield acceptable results, they are difficult to tune, i.e the tuning parameters can greatly vary between images in order to obtain the required STD. Recent work on sparse + low rank [17], [18] recovery have shown that the parameter μ, γ in (5) can recover the original decomposition when $\frac{\mu}{\gamma}$ is proportional to $\sqrt{\text{sparsity}/\text{rank}}$. In this paper, we take inspiration from such results and we extend them to the case of the LPR model: we consider the structure component as gradient-sparse and the texture component as low patch-rank, so that we can provide an automatic parameter selection method.

Contributions: The main contribution of this paper is to provide a novel algorithm to automatically tune the regularization parameters of the low patch-rank structure texture decomposition model, which adapts to the local content in the image. This allows us to construct a localized version of the LPR model with a reduced amount of parameters, e.g for an image of size 512×512 and using a window size of 64×64, using an overlap of 16, we reduce 121 parameters to a single parameter. The resulting algorithm is highly scalable as each operation can be parallelized efficiently. Finally, we demonstrate the robustness and effectiveness of our algorithm with numerical synthetic experiments (fig. 1) and comparative results (fig. 2) to other related methods (LPR and BNN) on real images.

II. Local LPR decomposition with automatic parameter selection

A. Localized LPR

In order to add localization of texture into the LPR model, we introduce the following subdivision with overlap of the image

$$\mathcal{Q}^o_{(n_1,m_1)}(f) = \begin{bmatrix} \mathcal{Q}(f)_{1,1} & \cdots & \mathcal{Q}(f)_{1,q_m} \\ \vdots & \ddots & \vdots \\ \mathcal{Q}(f)_{q_n,1} & \cdots & \mathcal{Q}(f)_{q_n,q_m}, \end{bmatrix}, \tag{3}$$

where o is the size of the overlap between adjacent blocks, (n_1, m_1) is the dimensions of the subdivision blocks $\mathcal{Q}(f)_{i,j}$. To simplify notations, we set $f_{i,j} = \mathcal{Q}(f)_{i,j}$ (and similarly $u_{i,j}$, $v_{i,j}$). Our model can be written as

$$\min_{\substack{u,v \\ f=u+v}} \sum_{i,j=1}^{q_n,q_m} \mu_{i,j} \|u_{i,j}\|_{TV} + \gamma_{i,j} \|\mathcal{P}(v_{i,j})\|_* , \tag{4}$$

where $\{\mu\}_{i,j=1}^{q_1,q_2}$ and $\{\gamma\}_{i,j=1}^{q_1,q_2}$ are the regularization parameters of the model. Furthermore, we set $\mathcal{Q}^{-1}$ as the pseudo-inverse mapping from the subdivision, where we use linear interpolation between frames to reconstruct overlapping regions.

B. Gradient-Sparse + Low Patch rank recovery

With their increase in number, it is not possible anymore to set manually the local regularization parameters of the localized LPR. We propose a novel method to automatically adjust the regularization parameters, which adapt to the local content in the image. The method is largely inspired from the problem of *sparse + low-rank* recovery of compressive sensing. Given a s-sparse matrix $\bar{u} \in \mathbb{R}^n$ such that $\|\bar{u}\|_0 = \#\{i,j \mid \bar{u}_{i,j} \neq 0\} \leq s$, a low-rank matrix $\bar{v} \in \mathbb{R}^n$ such that $\text{rank}(\bar{v}) \leq r$ and a linear map $\mathcal{A} : \mathbb{R}^n \to \mathbb{R}^m$, the aim of *sparse + low-rank* recovery is to recover the couple $(\bar{u}, \bar{v})$ from a measurement $b = \mathcal{A}(\bar{u} + \bar{v})$. Recent works [17], [18] have shown that the couple $(\bar{u}, \bar{v})$ can be recovered under some conditions via the minimization problem:

$$\min_{\substack{u,v \\ b=\mathcal{A}(u+v)}} \mu \|u\|_1 + \gamma \|v\|_* \tag{5}$$

when $\frac{\mu}{\gamma} = c\frac{\sqrt{r}}{\sqrt{s}}$, where c is a specified constant.

In [19], Chandrasekaran et al showed that the *sparse+low rank* matrix recovery problem could be solved with $\mathcal{A}=Id$ if the support space of the sparse component and the row+column space of the low-rank component are disjoint. Tanner and Vary's work [18] on the subject showed that if the incoherence between the sparse component and the low rank (LR) component and the operator $\mathcal{A}$ verifies a restricted isometry property (i.e. $\mathcal{A}$ behaves almost like an isometry on sparse + LR objects with incoherence), then the couple $(\bar{u}, \bar{v})$ can be recovered from (5), with $\frac{\mu}{\gamma} = \sqrt{\frac{2r}{s}}$. In a more general context, when the unknown is the concatenation (u, v) of a sparse vector and a LR matrix, it was shown in [17] that, for operators having the restricted isometry property (without incoherence between components, thus mostly specializing to random observation operators), the choice of $\frac{\mu}{\gamma} = \sqrt{\frac{r}{s}}$ is optimal for the family of low rank+sparse problems. In Section II-C, we propose to use this choice of parameters as a basis for automatic parameter selection in our localized LPR model. Indeed, in the LPR model the texture is interpreted as being of *low patch rank* and the structural component is constrained by the total variation which forces it to be *gradient-sparse*; the LPR model is a *gradient-sparse + low patch-rank* recovery problem, with $\mathcal{A} = Id$.

To test the validity of this parameter selection strategy, we conduct numerical experiments using synthetic 64×64 images where we control the gradient sparsity of the structure and the patch-rank of the texture (Fig. 1). The gradient sparsity is

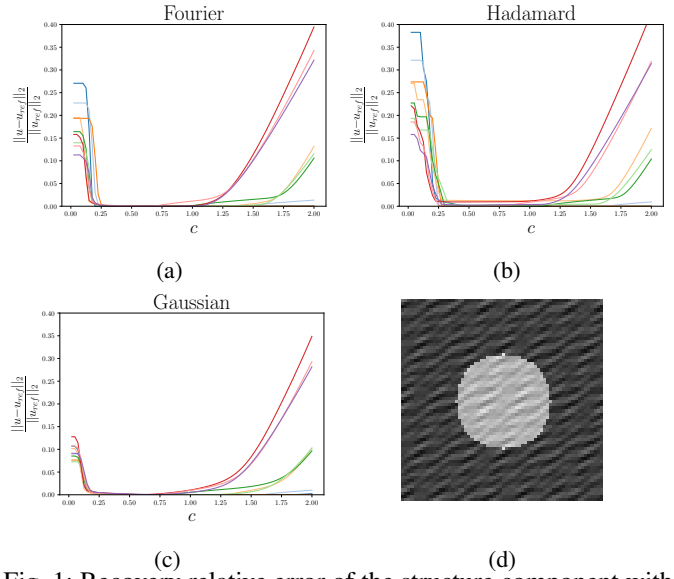

Fig. 1: Recovery relative error of the structure component with different gradient-sparsity $s\in\{105, 139, 173\}$ a¨nd patch-rank $r\in\{2, 4, 6\}$ via the LPR model with tuning parameters $\mu = \frac{c}{\sqrt{s}}$ and $\gamma = \frac{1}{\sqrt{r}}$. (a) Fourier texture, (b) Hadamard basis and (c) Gaussian basis. (d) Example of a synthetic test image with a fourier texture used in this experiment.

controlled by drawing a circle with a chosen radius, whereas the texture was synthesized using either a sparse Fourier texture or a Gaussian or Hadamard basis in the patch space. We then plot the relative error of reconstruction of (2) with $\frac{\mu}{\gamma} = c\sqrt{\frac{s}{r}}$, where s is the gradient-sparsity of the structure and r the patch-rank of the texture. We observe that for a given category of texture, a fixed $c \in [0.5, 0.75]$ minimizes the recovery error.

C. Local LPR with adaptive parameter tuning

Since the gradient-sparsity of the structure component and the patch-rank of the texture component cannot be distinguished beforehand, we propose to approximate them during the iterative steps of the ADMM and then to update the tuning parameters as follows:

$$\mu_{i,j} \approx \frac{c}{\sqrt{\|\nabla \tilde{u}_{i,j}\|_0}} \quad \text{and} \quad \gamma_{i,j} \approx \frac{1}{\sqrt{\text{rank}(\mathcal{P}(\tilde{v}_{i,j}))}}, \qquad (6)$$

where $\tilde{u}$ and $\tilde{v}$ are an approximation of the structural and textural components, and c is a constant that we can set manually. In practice, the gradient-sparsity and rank are estimated by enumerating the top 90% gradients and patch-singular values, denoted by $\|\cdot\|_{0,est}$ and $rank(\cdot)_{est}$ respectively. With this technique, we narrow down the number of required parameters to tune from $q_n \times q_m$ to a single parameter and each tuning parameter adapts to the local content in the image. In order to use the ADMM, we need to compute the proximal operator of the total variation, which can be quickly solved using FISTA [20] and the proximal operator of the nuclear norm, which is known as the singular value thresholding (SVT) operator [21]:

$$\text{prox}_{\|\cdot\|_*,\beta}(x) = SVT(x, \beta) = U \max(D - \beta I, 0)V^T, \qquad (7)$$

where $x = UDV^T$ is the singular value decomposition of x [22] and the maximum is taken elementwise. In practice, every (i, j)-operation can be performed simultaneously in parallel, making the method highly scalable.

Algorithm 1 (Our proposed method)
Notation: $z_{i,j} = \mathcal{Q}(z)_{i,j}$, $\mathcal{P}^{-1}$ the pseudo inverse of $\mathcal{P}$

$u^0 = f$, $v^0 = 0$, $y^0 = 0$
$\mu^0_{i,j} = \frac{c}{\sqrt{\|\nabla f_{i,j}\|_0}}$, $\gamma^0_{i,j} = \frac{1}{p}$
while not converged **do**
  for each $(i, j) \in [\![1, q_n]\!]\times[\![1, q_m]\!]$ **do**
    $u^{k+1}_{i,j} = \text{prox}_{TV, \frac{\mu^k_{i,j}}{\rho}}((f - v^k - y^k)_{i,j})$
    $v^{k+1}_{i,j} = \mathcal{P}^{-1}(\text{SVT}(\mathcal{P}(f - u^{k+1} - y^k)_{i,j}, \frac{\gamma^k_{i,j}}{\rho}))$
    if $k = 0$ mod M **then**
      $\mu^{k+1}_{i,j} = \frac{c}{\sqrt{\|\nabla u^{k+1}_{i,j}\|_{0,est}}}$
      $\gamma^{k+1}_{i,j} = \frac{1}{\sqrt{\text{rank}(v^{k+1}_{i,j})_{est}}}$
    end if
  end for
  $u^{k+1}, v^{k+1} = \mathcal{Q}^{-1}(\{u^{k+1}_{i,j}\}_{i,j}), \mathcal{Q}^{-1}(\{v^{k+1}_{i,j}\}_{i,j})$
  $y^{k+1} = y^k + (u^{k+1} + v^{k+1} - f)$
end while

III. Experimental results

We present some decomposition results (fig. 2), where we compare our method to the Low Patch Rank (LPR) and Block Norm Normalization (BNN) methods. The source code of our algorithm 1 and numerical experiments (fig. 1) can be found in the git repository [23]. In our decomposition results, the patch operator $\mathcal{P}$ was parameterized with a patch size p=5 and the subdivision $\mathcal{Q}$ of the image was performed with (n_1,m_1)=$(64, 64)$ and an overlap o=16. Finally, our tuning parameter was set to c=0.65 for every image and in order to achieve comparative results with our method, we tuned the LPR and BNN models for each image such that the output textural components are of similar magnitude by requiring $|\,\|v_{other}\|_2 - \|v_{proposed}\|_2\,|$<0.1.

As seen in our results, our method achieves better decomposition than the original LPR and BNN. For the same amount of texture, our structure component is sharper and while BNN captures well stripes-like textures, we observed that this tends to force a lot of structural details such as facial features into the textural component. Moreover, fine grain texture such as the floor in the Barbara image is left out compared to our method (see fig. 3). Finally, we observe that our localization of the LPR model improves it significantly with a gain in sharpness with a lot less structural component being present in the texture (e.g the hat in the zoom of the middle image, fig. 2).

Furthermore, compared with other methods, our method requires very little tuning: indeed, when we set any $c\in[0.5, 0.75]$ we observed that our method achieves a good image decomposition for these images (and more, available in [23]). To illustrate the robustness of our method: in Fig. 2, our method

Fig. 2: Comparison between different methods. From left to right: original image, LPR, BNN and our proposed method.

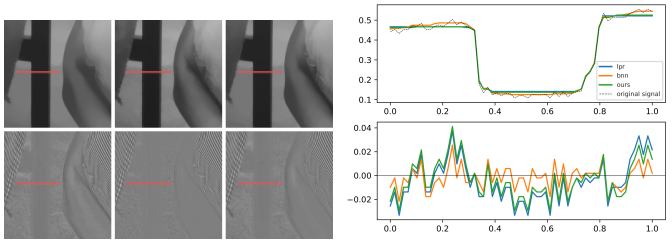

(a) (b)

Fig. 3: 1-dimensional sample taken from the Barbara image with different decompositions. a) Zoom on the table leg for the different decomposition methods (from left to right: LPR, BNN and ours). b) 1-D graph of the area highlighted in red with different decomposition; top graph: structure component, bottom graph: texture component. We observe that the cartoon component of BNN tends to pursue the original signal, while LPR and ours are more piecewise constant. This leads the BNN to capture less texture in the region surrounding the table leg in the image.

was performed with a fixed c=0.65 whereas the other methods required changes of up to 60% and 53% in the parametrization for LPR and BNN methods respectively. Furthermore, since our method is performed locally simultaneously, we can significantly accelerate the process by parallelizing the computing using a graphic processing unit.

IV. Conclusion

We presented an efficient parameter selection strategy for the gradient sparse plus low patch rank model, validated by experiments. There are still some open questions which should be investigated in the future. On the one hand, from a theoretical point of view, the *gradient-sparse + low patch-rank* recovery problem has yet to be studied. Fundamentally, in the *sparse + low rank* recovery problem, sparse and LR matrices cannot be recovered by (5) when they are not sufficiently incoherent one to the other: it is not clear how this translates on the type of structure-texture decomposition that can be recovered using the LPR model. On the other hand, the convergence of the scheme we used to update our parameters should be explored further.

Up to now, tuning decomposition models has remained largely try-and-error and our tuning methodology could also benefit other sparsity/low rank prior based decomposition models such as BNN in order to reach an optimal decomposition.

Acknowledgment

This work was supported by the French National Research Agency (ANR) under reference ANR-20-CE40-0001 (EFFIREG project) and ANR-18-CE92-0050 (SUPREMATIM project). Experiments presented in this paper were carried out using the PlaFRIM experimental testbed, supported by Inria, CNRS (LABRI and IMB), Université de Bordeaux, Bordeaux INP and Conseil Régional d'Aquitaine (see https://www.plafrim.fr). We express our gratitude to the reviewers for their time and helpful feedback.

References

[1] L. I. Rudin, S. Osher, and E. Fatemi, "Nonlinear total variation based noise removal algorithms," *Physica D: nonlinear phenomena*, vol. 60, no. 1-4, pp. 259–268, 1992.

[2] Y. Meyer, *Oscillating patterns in image processing and nonlinear evolution equations: the fifteenth Dean Jacqueline B. Lewis memorial lectures*. American Mathematical Soc., 2001, vol. 22.

[3] L. A. Vese and S. J. Osher, "Modeling textures with total variation minimization and oscillating patterns in image processing," *Journal of scientific computing*, vol. 19, pp. 553–572, 2003.

[4] S. Alliney, "A property of the minimum vectors of a regularizing functional defined by means of the absolute norm," *IEEE transactions on signal processing*, vol. 45, no. 4, pp. 913–917, 1997.

[5] J.-F. Aujol, G. Gilboa, T. Chan, and S. Osher, "Structure-texture image decomposition—modeling, algorithms, and parameter selection," *International journal of computer vision*, vol. 67, pp. 111–136, 2006.

[6] J.-F. Aujol, G. Aubert, L. Blanc-Féraud, and A. Chambolle, "Image decomposition into a bounded variation component and an oscillating component," *Journal of Mathematical Imaging and Vision*, vol. 22, no. 1, pp. 71–88, 2005.

[7] F. Zhou, Q. Chen, B. Liu, and G. Qiu, "Structure and texture-aware image decomposition via training a neural network," *IEEE Transactions on Image Processing*, vol. 29, pp. 3458–3473, 2019.

[8] Y. Fang, H. Fan, L. Sun, Y. Guo, and Z. Ma, "From tv-l 1 to gated recurrent nets," in *ICASSP 2019-2019 IEEE International Conference on Acoustics, Speech and Signal Processing (ICASSP)*. IEEE, 2019, pp. 2212–2216.

[9] B. Shi, W. Xu, and X. Yang, "Ctdnet: cartoon-texture decomposition-based gray image super-resolution network with multiple degradations," *JOSA B*, vol. 40, no. 12, pp. 3284–3290, 2023.

[10] C. Zheng, D. Shi, and W. Shi, "Adaptive unfolding total variation network for low-light image enhancement," in *Proceedings of the IEEE/CVF international conference on computer vision*, 2021, pp. 4439–4448.

[11] J.-L. Starck, M. Elad, and D. L. Donoho, "Image decomposition via the combination of sparse representations and a variational approach," *IEEE transactions on image processing*, vol. 14, no. 10, pp. 1570–1582, 2005.

[12] M. J. Fadili, J.-L. Starck, J. Bobin, and Y. Moudden, "Image decomposition and separation using sparse representations: An overview," *Proceedings of the IEEE*, vol. 98, no. 6, pp. 983–994, 2009.

[13] H. Zhang and V. M. Patel, "Convolutional sparse and low-rank coding-based image decomposition," *IEEE Transactions on Image Processing*, vol. 27, no. 5, pp. 2121–2133, 2017.

[14] H. Schaeffer and S. Osher, "A low patch-rank interpretation of texture," *SIAM Journal on Imaging Sciences*, vol. 6, no. 1, pp. 226–262, 2013.

[15] S. Boyd, N. Parikh, E. Chu, B. Peleato, J. Eckstein *et al.*, "Distributed optimization and statistical learning via the alternating direction method of multipliers," *Foundations and Trends® in Machine learning*, vol. 3, no. 1, pp. 1–122, 2011.

[16] S. Ono, T. Miyata, and I. Yamada, "Cartoon-texture image decomposition using blockwise low-rank texture characterization," *IEEE Transactions on Image Processing*, vol. 23, no. 3, pp. 1128–1142, March 2014.

[17] Y. Traonmilin, R. Gribonval, and S. Vaiter, "A theory of optimal convex regularization for low-dimensional recovery," *arXiv preprint arXiv:2112.03540*, 2022.

[18] J. Tanner and S. Vary, "Compressed sensing of low-rank plus sparse matrices," *Applied and Computational Harmonic Analysis*, 2023.

[19] V. Chandrasekaran, S. Sanghavi, P. A. Parrilo, and A. S. Willsky, "Rank-sparsity incoherence for matrix decomposition," *SIAM Journal on Optimization*, vol. 21, no. 2, pp. 572–596, 2011.

[20] A. Chambolle and T. Pock, "A first-order primal-dual algorithm for convex problems with applications to imaging," *Journal of mathematical imaging and vision*, vol. 40, pp. 120–145, 2011.

[21] J.-F. Cai, E. J. Candès, and Z. Shen, "A singular value thresholding algorithm for matrix completion," *SIAM Journal on optimization*, vol. 20, no. 4, pp. 1956–1982, 2010.

[22] L. N. Trefethen and D. Bau, *Numerical linear algebra*. Siam, 2022, vol. 181.

[23] A. Guennec, J.-F. Aujol, and Y. Traonmilin, "Structure-texture-decomposition-gs-lpr," https://github.com/aguennecjacq/Structure-Texture-Decomposition-GS-LPR, 2023.